Journal of Nuclear Materials 390–391 (2009) 1135–1137

Contents lists available at ScienceDirect

Journal of Nuclear Materials

journal homepage: www.elsevier.com/locate/jnucmat

Reactivity of rhodium during co-deposition of rhodium and carbon

Laurent Marot [a,*], Roland Steiner [a], Gregory De Temmerman [b], Peter Oelhafen [a]

[a] Department of Physics, University of Basel, Klingelbergstrasse 82, CH-4056 Basel, Switzerland
[b] EURATOM/UKAEA Fusion Association, Culham Science Centre, UK

ARTICLE INFO

PACS:
81.15.Cd
52.40.Hf
52.55.Fa
78.20.Ci

ABSTRACT

The detailed characterizations of rhodium/carbon films prepared by co-deposition using a dual magnetron sputtering have been carried out on silicon substrates at room temperature. Effects of the carbon incorporated in the film on the chemical bonding state, optical reflectivity and crystallinity were investigated using XPS, reflectivity measurements, XRD and SEM. The incorporation of carbon changes the films' crystallinity and thus producing amorphous films. The reflectivity of the films decreases linearly as the rhodium concentration decreases. It is important to note that no chemical bonding was observed between rhodium and carbon whatever the deposition conditions, even at high deposition temperature. Concerning the reactivity of rhodium films with oxygen, after long term storage in air the rhodium surface is covered with a thin rhodium oxide (few nanometers). However, for these films no variation of the optical reflectivity was observed after long air storage.

1. Introduction

Rhodium is considered to be one of the most promising materials for the first mirrors [1–3] of the diagnostic systems of the International Thermonuclear Experimental Reactor, due to its high reflectivity in the visible range and its low sputtering yield. It is thus envisaged to use rhodium coatings on polished metallic substrates. The preparation of such mirrors was reported in our previous papers [4,5]. To ensure the reliability of these components in a nuclear fusion environment it is necessary to determine their chemical stability and in particular the reactivity of rhodium towards typical impurities in a tokamak such as carbon, oxygen, beryllium and tungsten. In fact, any change in the surface composition will affect the mirror reflectivity and in turn the signal measured by the diagnostic system.

In this work, we will focus primarily on rhodium films deposited by a dual magnetron sputtering in order to investigate the influence of carbon on chemical composition, crystallinity and on the optical properties.

2. Experimental part

Co-deposition of rhodium and carbon were performed in a high vacuum chamber pumped down to a base pressure of about 2×10^{-4} Pa using a conventional pumping system [4]. The dual target arrangement consists of an internal Rh target put in the centre of an external carbon target which has the form of a ring (Fig. 1). The inner Rh target was driven by a pulsed-DC power with a power of 25 W, the outer one by a second, identically pulsed-DC power supply. The relative concentrations of Rh and C in the film were changed by modifying the power applied to the carbon target in the range of 15–250 W. The pure rhodium and carbon film were deposited using only one target with a power of 25 and 250 W, respectively.

Depositions were carried out on silicon (100) substrates. The deposited films' thicknesses were in a range of 110–150 nm as determined by cross section SEM observations. The substrate was placed at a distance of 10 cm from the target. In addition, the substrate holder allowed the deposition at elevated temperatures by means of resistive heating. After deposition, the samples were transferred from the high vacuum plasma chamber to the ultrahigh vacuum (UHV) chamber housing a photoelectron spectrometer (XPS) without breaking the vacuum.

The UHV working pressure was about 5×10^{-9} Pa. The electron spectrometer is equipped with a hemispherical analyser (Leybold EA10/100 MCD) and a non-monochromatized Mg Kα X-ray source was used ($h\nu$ = 1253.6 eV) for core level spectroscopy. The typical resolution is 0.8 eV for the XPS measurements. The binding energy scale was calibrated using the Au 4f7/2 line of a cleaned gold sample at 84.0 eV. Moreover, large scale XPS-spectra from 0 to 1000 eV did not show any other peak than those due to rhodium and carbon. The acquisition mode was set to CAE (constant analyser energy) with 29 eV pass energy (0.05 eV step size) and a normal electron escape angle. As all our samples were verified to be stable in UHV and under X-ray irradiation, the signals could be collected during a time long enough to make the electronic signal noise

* Corresponding author.
E-mail address: laurent.marot@unibas.ch (L. Marot).

0022-3115/$ - see front matter © 2009 Elsevier B.V. All rights reserved.
doi:10.1016/j.jnucmat.2009.01.266

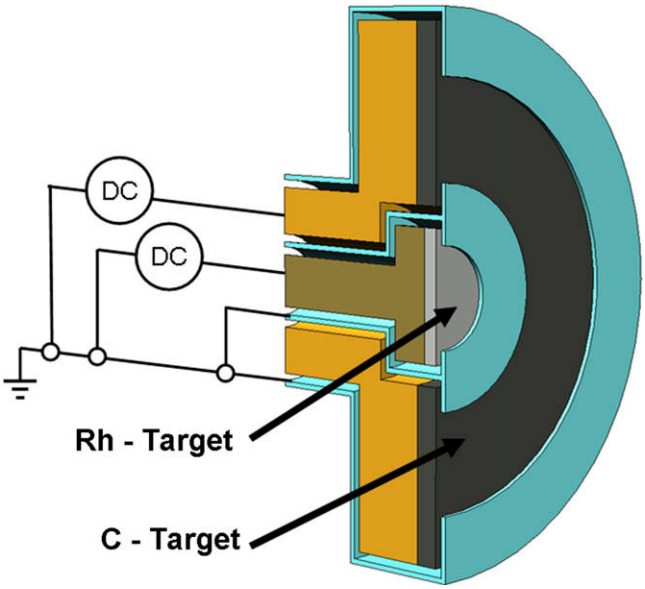

Fig. 1. Schematic representation of dual magnetron system.

negligible: in this way, no signal smoothing appears necessary when fitting the line-shapes with high accuracy.

The morphology of the films was investigated by top view SEM (Hitachi S-4800 field emission at 5 kV). X-rays diffractograms (XRD) were recorded using a SIEMENS D5000 instrument with monochromatic Cu Kα radiation (40 kV and 30 mA) at a grazing incidence of 5°. All XRD patterns were obtained with scan steps of 0.02° and with 8 s of acquisition time in the range of 25°–90°.

Moreover, the ellipsometric parameters' angles (Ψ, Δ) were measured by means of a spectral ellipsometer (Sentech SE 850) in the range 300–2300 nm for angles of incidence of 45°, 55° and 65°. The fit of these six data sets (fitting routine SpectraRay) using a fixed refractive index and absorption model was performed to obtain the optical constants of the film as a function of the wavelength. The reflectivity of the film at normal incidence was then recalculated using these optical constants.

3. Results and discussion

Films have been deposited at room temperature (RT) with different powers applied to the carbon target. Fig. 2 shows the Rh3d and C1s core level measured in-situ after each deposition step. Fittings of the data were performed using Doniach–Sunjic functions [6], after a Shirley background subtraction [7] with the help of UNIFIT for Windows (Version 3.2) software [8]. A convolution of Lorentzian and Gaussian line-shapes was used to fit the individual peaks. The asymmetric peak shapes were used for metal lines. The $Rh3d_{5/2}$ peaks position move from 307.0 to 307.21 eV for 100% and 36.8% of rhodium in the film, respectively. Only for 3.3% of rhodium the position of the $Rh3d_{5/2}$ peak is 307.7 eV, this shift is typical for metal cluster imbedded in amorphous films [9], A deconvolution with two lorentzian-gaussian curves performed, after a Shirley background subtraction, (not shown here), reveals two components of the C1s line. One line is associated to C–O for a binding energy of 286 eV [10,11] the percentage of this compound representing no more than 5% for all these samples. The second line is a pure amorphous carbon phase (a-C), with a binding energy of 284.64 eV for pure carbon deposition. The calculated reflectivity of relevant films is plotted in Fig. 3. In the case of pure rhodium films, the reflectivity is the same as the theoretical one [4]. The reflectivity of the other films decreases linearly as the rhodium concentration decreases. For pure amorphous carbon the reflectivity shows interference phenomena. Fig. 4 shows XRD measurements at a glancing incidence of relevant films for the range 25°–50° only, in order to simplify / facilitate the observation. The intensity of the rhodium peaks decreases as the percentage of rhodium decreases and for less than 85.4% of rhodium no more peaks are observable.

Deposition were also carried out at 320 and 500 °C with a constant power of 160 W applied to the carbon target. For these two temperatures the rhodium concentration in the films is 48.8% and 45.5%, respectively. XPS measurements are similar to the one deposited at RT for the 57.2% of rhodium in the film. The XRD patterns for both temperatures revealed rhodium phases like in our previous pattern for pure rhodium [4]. In comparison to RT (Fig. 4), where the Rh (200), Rh (220) and Rh (311) peaks disap-

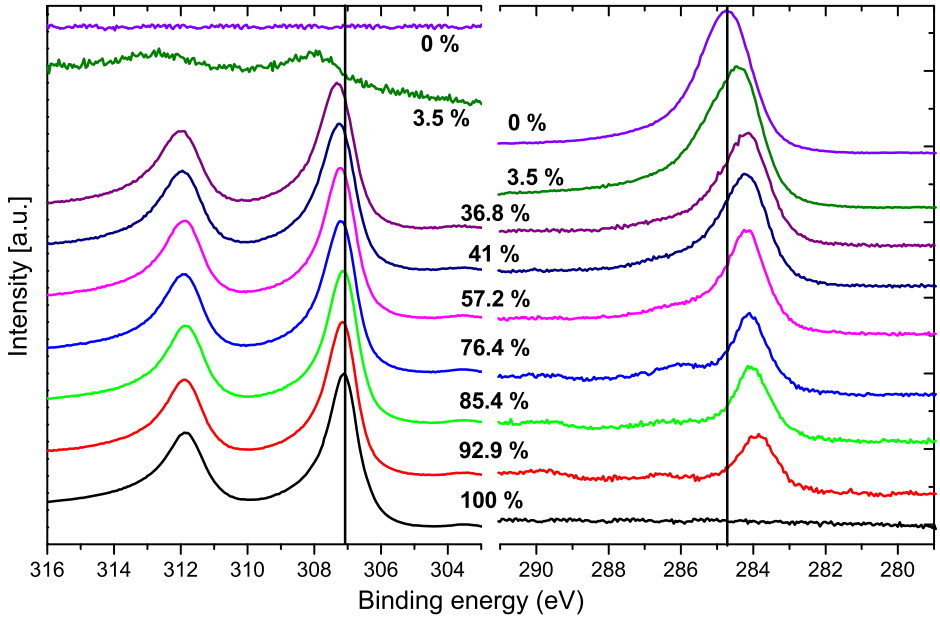

Fig. 2. Rh3d and C1s core level spectra measured by in-situ XPS on rhodium films deposited on silicon substrates with various concentration of rhodium. In all cases, the spectra have been normalized for comparison. The vertical lines are present as eye guide.

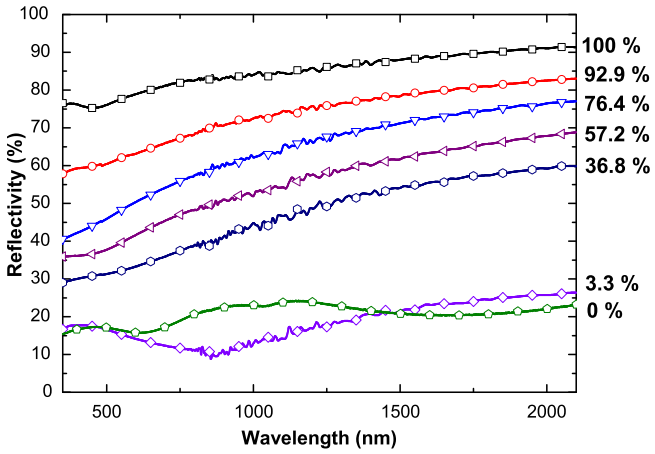

Fig. 3. Evolution of the reflectivity calculated by spectroscopic ellipsometry measurements of rhodium films deposited at RT on silicon for various rhodium concentration.

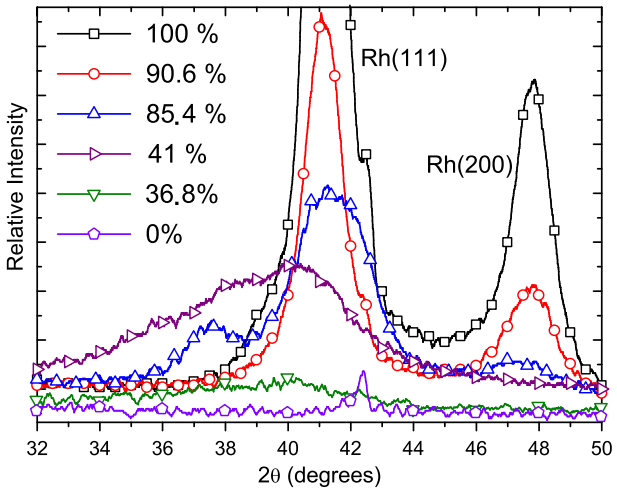

Fig. 4. X-ray diffraction pattern of rhodium films deposited at RT on silicon with various oxygen rhodium concentration.

pears for less than 85.4% of rhodium, all these peaks are always present for the heating deposition. For these depositions the rhodium is always crystalline. Top view SEM images for these three deposition temperatures (not shown here) revealed a granular structure for the film deposited at elevated temperature. The calculated reflectivity of these films is 11% and 16% less than the films deposited at RT for a temperature of 320 and 500 °C, respectively.

3.1. The effect of oxygen

In the same setup, the preparation and detailed characterization of sub-stoichiometric rhodium oxide films prepared by magnetron sputtering with different oxygen gas flow ratio have been reported in our previous work [12]. Sub-stoichiometric rhodium oxide films are formed by deposition of rhodium in an oxygen gas process. At room temperature, for low oxygen ratio, the main component of the film is metallic rhodium and with more oxygen in the gas process only a sub-stoichiometric rhodium oxide film is present. In contrast with 300 °C deposition and even with pure oxygen plasma, metallic rhodium is always observed. The reflectivity of these films is controlled by the presence of metallic rhodium in the film. For the pure rhodium metal, the reflectivity is comparable to the reference values (>70–80%). In the case of pure oxide film the reflectivity drops below 40%.

Moreover, after long term storage in air, the surface of pure rhodium mirrors is covered with adsorbed molecules (oxygen, carbon) and a thin rhodium oxide layer is formed on the surface [5]. For all the samples used in this study, no variation of the optical reflectivity was observed after long air storage of the samples. Annealing cycles have been performed 10 times for 5 h at 200 °C in air [5]. No evolution of the reflectivity was observed in the range of 250–2500 nm. The XPS measurement after annealing cycles is quite similar to those made after air storage and revealed a thin Rh_2O_3 oxide film on the surface.

4. Conclusion

Different rhodium/carbon films have been characterized by XPS, XRD and optical measurements. No chemical bonding was observed between rhodium and carbon whatever the deposition conditions, even at high deposition temperature. The reflectivity of the films decreases linearly as the rhodium concentration decreases and no rhodium crystalline phase is measured for less than 85.4% of rhodium. All these properties, i.e. no formation of carbide and no significant oxidation in air, show the advantages of this material in comparison to molybdenum mirrors [13].

Acknowledgements

The financial support of the Swiss Federal Office of Energy and of the Federal Office for Education and Science is gratefully acknowledged.

References

[1] ITER Physics Basis, Nucl. Fus. 39–12 (1999) 2541.
[2] A. Litnovsky, V.S. Voitsenya, A. Costley, T. Donné, Nucl. Fus. 47 (2007) 833.
[3] M.J. Walsh, M. Beurskens, P.G. Carolan, M. Gilbert, R.B. Huxford, M. Loughlin, A.W. Morris, V. Riccardo, C. Walker, Y. Xue, Rev. Sci. Instrum. 77 (2006) 10E525.
[4] L. Marot, G. De Temmerman, V. Thommen, D. Mathys, P. Oelhafen, Surf. Coat. Technol. 202 (2008) 2837.
[5] L. Marot, G. De Temmerman, G. Covarel, A. Litnovsky, P. Oelhafen, Rev. Sci. Instrum. 78 (2007) 103507.
[6] S. Doniach, M. Sunjic, J. Phys. C: Solid State Phys. 3 (1970) 285.
[7] D.A. Shirley, Phys. Rev. B 5 (1972) 4709.
[8] R. Hesse, T. Chassé, R. Szargan, Fresen. J. Anal. Chem. 365 (1999) 48.
[9] C. Bittencourt, A. Felten, B. Douhard, J.-F. Colomer, G. Van Tendeloo, W. Drube, J. Ghijsen, J.-J. Pireaux, Surf. Sci. 601 (2007) 2800.
[10] C.D. Wagner, W.M. Riggs, L.E. Davis, J.F. Moulder, Handbook of X-ray Photoelectron Spectroscopy, Physical Electronics Division, MN, USA, 1979, p. 261.
[11] H. Estrade-Szwarckopf, Carbon 42 (2004) 1713.
[12] L. Marot, G. De Temmerman, Peter Oelhafen, Surf. Sci. 602 (2008) 3375.
[13] A. Litnovsky, G. De Temmerman, K. Vukolov, P. Wienhold, V. Philipps, O. Schmitz, U. Samm, G. Sergienko, P. Oelhafen, M. Büttner, I. Orlovskiy, A. Yastrebkov, U. Breuer, A. Scholl, Fus. Eng. Des. 123 (2007) 82.